WS_2 nanotubes containing single-walled carbon nanotube bundles

R. L. D. Whitby, W. K. Hsu, P. C. P. Watts, H. W. Kroto, and D. R. M. Walton[a)]
School of Chemistry, Physics and Environmental Science, University of Sussex, Brighton BN1 9QJ, United Kingdom

C. B. Boothroyd
Department of Materials Science and Metallurgy, University of Cambridge, Pembroke Street, Cambridge CB2 3QZ, United Kingdom

(Received 31 August 2001; accepted for publication 15 October 2001)

Single-walled carbon nanotubes (SWCNs) encapsulated in multiwalled WS_2 nanotubes are produced by pyrolyzing a mixture of WO_{3-x} and SWCNs in N_2/H_2S atmosphere. © *2001 American Institute of Physics.* [DOI: 10.1063/1.1425467]

Recently, binary phase WS_2–C nanotubes [Fig. 1(a)] have been successfully produced by pyrolyzing WO_x-coated multiwalled carbon nanotubes (MWCNs) at 900 °C in the presence of a gaseous H_2S/N_2 mixture.[1,2] These nanotubes exhibit strong high resolution transmission electron microscopy (HRTEM) fringe contrast between WS_2 (i.e., dark) and C (i.e., light), and their characterization by HRTEM and energy dispersive x-ray (EDX) techniques was straightforward. In Fig. 1(a), the basal planes of MWCNs (i.e., a layered structure) are clearly present and lie parallel to the WS_2 sidewall fringes (i.e., outermost layer). We found that when the WS_2 coating is thick (>2 layers), HRTEM details of the layered structure of the MWCNs are obscured due to interference from the WS_2 lattice fringe. Electron diffraction (ED) analysis of WS_2–C nanotubes revealed a complex hexagonal pattern consisting of helical WS_2 and zigzag-edged MWCN spot arrays.[1,2] In this letter, we investigate the encapsulation of single-walled carbon nanotubes (SWCNs) by multiwalled WS_2 nanotubes using a similar method of production.[1,2]

The SWCNs were made by the arc discharge between a Ni/Y-doped graphite anode and a C cathode, described by Journet *et al.*[3] Arc-generated soot (~50 mg) was placed in a Soxhlet apparatus and extracted with boiling toluene (100 cm^3) over 3 h in order to remove soluble fullerenes. The residual soot contains SWCNs, amorphous carbon, and Ni/Y encapsulated carbon particles [Fig. 1(b)]. Several features in the mixture can be distinguished. The SWCNs aggregate and form bundles [inset, Fig. 1(b)] ~5–20 nm in diameter and 2–5 μm in length. The individual bundles consist of ~3–20 SWCNs [inset, Fig. 1(a)] coated with amorphous carbon, which are interconnected via metal particles, similar to a network [Fig. 1(b)]. The diameters of the SWCNs are ~1–2 nm; the individual SWCNs are slightly twisted in the bundle aggregates.

A mixture of the residual soot, H_2WO_4 (250 mg), and liquid ammonia (5 cm^3) at −78 °C was stirred continuously, allowed to attain room temperature, then heated at 350 °C for 15 min under a continuous flow of air (50 cm^3/min). The reason for oxidizing the mixture at 350 °C is to convert H_2WO_4 into WO_3 and to remove the amorphous carbon coating from the SWCNs. The sample at this stage still consists of SWCN bundles and Ni/Y encapsulated carbon particles, together with large numbers of WO_3 particles (5–40 nm in diameter). HRTEM also revealed that (a) the network structure of SWCNs had disappeared; (b) the numbers of Ni/Y encapsulated carbon particles and SWCN bundles were reduced significantly, and (c) the surfaces of SWCN bundles were fairly clean. However, amorphous coatings were still present. Due to the rapidity of the damage caused by the electron beam to the SWCNs, we were unable to identify the amorphous coating by EDX analysis. The amorphous coating of the SWCN bundles is either residual carbon, due to incomplete oxidation, or amorphous WO_{3-x}, formed during $H_2WO_4 \rightarrow WO_3$ conversion.

The oxidized mixture was subsequently heated at 900 °C in a gaseous mixture of 3:1 N_2/H_2S (flow rate of 50 cm^3/min) for 10 min. HRTEM (CM-200, JEOL 4000-EX-II) showed that the products, after H_2S pyrolysis, consisted of (a) a small number (~5%) of SWCN bundles; (b) dark multiwalled particles (~50%–60%, 5–40 nm in diameter), and (c) dark multiwalled nanotubes [~30%–40%, 10–20 nm in diameter, 5–15 μm in length, Fig. 1(c)]. Ni/Y encapsulated carbon particles were absent. The HRTEM and EDX showed that materials (b) and (c) exhibit 6.2 Å *d* spacing along the *c* axis, and consist of W and S (i.e., WS_2 nanotubes and particles), together with a trace of O. It is worth noting that in

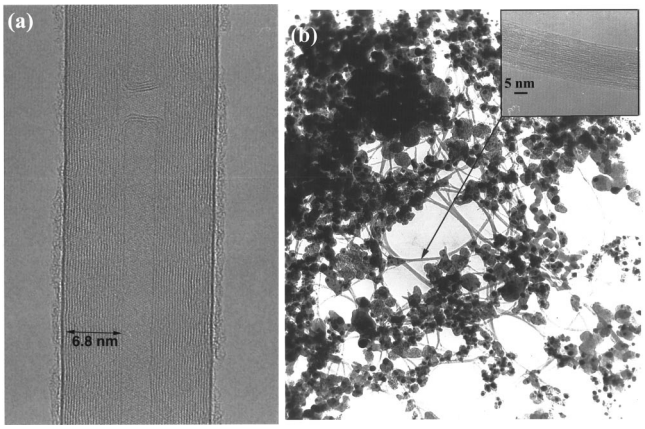

FIG. 1. (a) HRTEM image of a single WS_2 layer coating a multiwalled carbon nanotube. (b) Single-walled carbon nanotubes produced by the Ni/Y–graphite arc method. Individual SWCN bundles are shown in the inset.

a)Electronic mail: d.walton@sussex.ac.uk

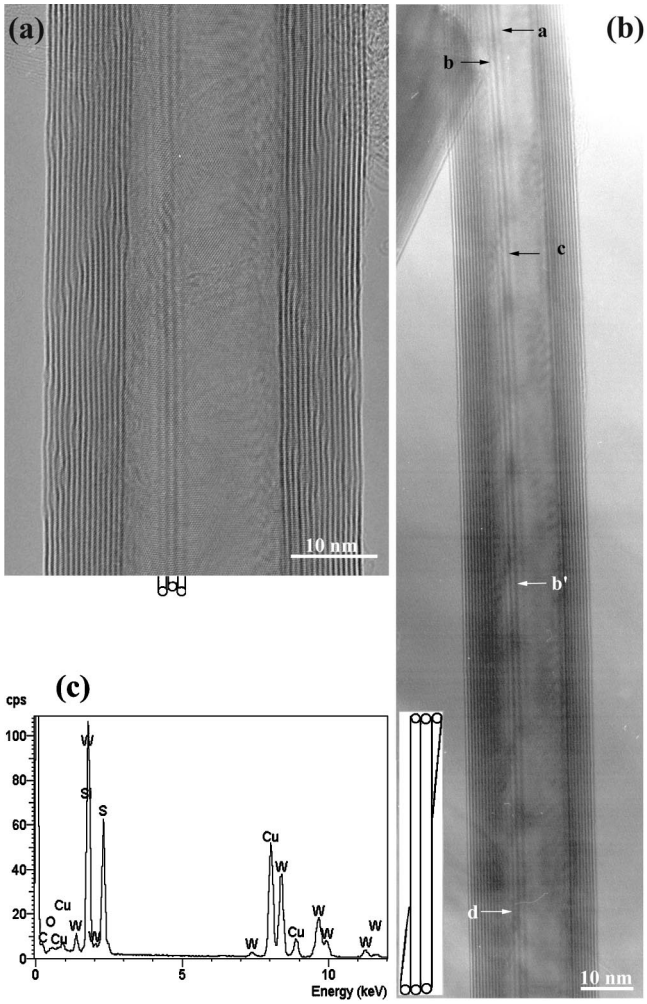

FIG. 2. (a) HRTEM image of a 15 walled WS_2 nanotube containing SWCNs. (b) HRTEM image of a 10 walled WS_2 nanotube containing SWCNs. (c) EDX analysis of a multiwalled WS_2 nanotube containing SWCNs.

this experiment the individual SWCN bundles did not coalesce into larger MWCNs upon heating at 900 °C (i.e., graphitization), as reported previously.[4]

During HRTEM studies, we noticed that the 6.2 Å spacing of WS_2 became visible above 200 K magnification (0.16 nm resolution, JEOL, 4000-EX). To observe the 3.4 Å spacing in MWCNs, the HRTEM must be operated above 250 K. We frequently observed additional tube-like fringes between the WS_2 side-wall fringes. Typical examples are shown in Figs. 2(a) and 2(b). To the best of our knowledge, these additional tube-like fringes have not been seen previously WS_2 nanotubes.[5–8] The tube-like fringes do not arise from lattice fringe interference of multiwalled WS_2 tubes (due to different chiralities of individual WS_2 shells) or from SWCN attachment to WS_2 nanotube external surfaces. The interference of individual WS_2 shells will only produce localized complex fringes,[5–8] not a continuous tube-like fringe. In order to exclude the possibility that the SWCNs are attached to the outer surfaces of WS_2 tubes, HRTEM studies were conducted at 400 keV [JEOL, 4000-EX, Fig. 2(a)] and at 200 keV [Philips, CM-200, Fig. 2(b)], respectively. They showed that the lifetime stability of the SWCNs under irradiation at 200 keV was ~5 min.[9] The higher the accelerating voltage, the greater the ''atomic knock-on damage'' to the SWCNs.[9] The heating effect caused by electron irradiation (i.e., inelastic scattering) of the samples is negligible (<100 °C for both 200 and 400 keV).[10] No changes in any additional tube-like fringes were found when irradiation (200 and 400 keV) was extended to 10 min. This operation time includes magnification adjustment and beam focusing (~2–3 min) and taking a series of defocused pictures (~7–10 min). We therefore conclude that the additional tube-like fringes seen between WS_2 side-wall fringes correspond to SWCNs. That is, the SWCNs are encapsulated in WS_2 nanotubes based on the following observations: (a) the diameter of tube-like fringes is ~1–2 nm, similar to in as-grown SWCNs; (b) the structure of SWCNs remains intact after 10 min electron irradiation, possibly due to protection of the WS_2 shell; (c) a trace of C was detected by EDX.

In order to exclude the detection of C arising from the holey carbon support film and from condensation of carbon vapor from the support film (caused by beam irradiation), we carried out EDX analyses (Philips, CM-200) as follows. First, the EDX probe (~200 000 spectrum counts) was focused onto the carbon film and onto the vacuum, respectively, which allows us to determine the C-signal intensity. No distinguishable C peak was observed in the vacuum. The EDX probe was also focused onto a protruding empty WS_2 tube (~3 μm from the film) with 100 K magnification (smallest aperture at spot size 4, beam spot ~20 nm) for 1 min. This experiment allows us to determine whether C-vapor condensation on WS_2 nanotubes occurs over time (5 min). However, no C signal was detected. A WS_2 nanotube containing internal SWCN bundle fringes was selected and subsequently analyzed by EDX. C was observed to be present, together with W, S and a trace of O [Fig. 2(c)], with the presence of O possibly arising from WO_{3-x} coating of the SWCNs.

In Fig. 2(b), straight line fringes are located near the side walls of the WS_2 nanotube. The individual fringes are labeled a, b, c, b′ and d, respectively [Fig. 2(b)]. The spacing between a and c, b and c, c and b′ and b and d is ~1.5, 1.3, 1.3 and 1.3 nm, respectively. According to the HRTEM image [Fig. 1(b)], the diameter of individual SWCNs is ~1–2 nm. If these straight-line fringes correspond to trapped SWCNs, then the number of trapped SWCNs in the WS_2 nantube is four [Fig. 2(b)] based on the following observations. The diameter of the first SWCN is ~1.5 nm, corresponding to a–c spacing. The second SWCN diameter is ~1.3 nm, corresponding to b–c spacing. The third SWCN diameter is ~1.3 nm, corresponding to c–b′ spacing. The fourth SWCN diameter is ~1.3 nm, corresponding to b–d spacing. It should be noted that the first SWCN fringe (i.e., a–c spacing) gradually vanishes near position b′. Meanwhile, the fourth SWCN fringe (i.e., b–d spacing) begins to emerge near the same area, position b′. The SWCN bundles often become twisted in this way. It is therefore possible that a–c and b–d fringes arise from the same SWCN, which is twisted about the second (b–c spacing) and third (c–b′) ones [inset, Fig. 2(b)]. Thus, the actual number of trapped SWCNs in the WS_2 nanotube is 3. It is important to point out that the diameter of trapped SWCNs varies slightly with the beam defocus depth. This phenomenon is due to trapped SWCNs and WS_2 nanotubes being situated at different levels. There-

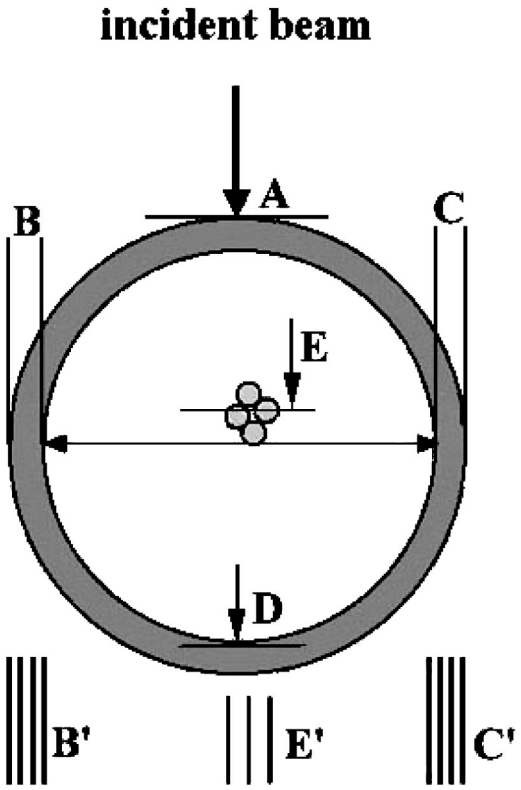

FIG. 3. Formation of trapped SWCN fringes inside WS_2 nanotubes.

fore, when the HRTEM beam focuses accurately onto the WS_2 nanotube, the trapped SWCN fringes are slightly obscured, which makes measurement of the actual SWCN diameters less accurate. All trapped SWCN diameters were measured by adjusting the beam defocus depth to 400–500 nm, allowing the SWCN fringes to be optimized. Figure 3 shows a schematic of a plausible arrangement of trapped SWCNs. The electron beam passes through the upper surface of the WS_2 nanotube (point **A**). The region where there is a greater number of atoms, due to concentric nanotube cylinders, is aligned with the electron beam (points **B** and **C**), thus creating a thick basal plane fringe (6.2 Å spacing) in the HRTEM image (**B**′ and **C**′). The beam then passes through the rear of the nanotube (point **D**), and the trapped SWCNs cause additional beam scattering within the WS_2 nanotube (Fig. 3, **E**). Stepwise defocusing was applied to sharpen details of the image within the WS_2 nanotube body (Fig. 3, defocus steps between **A** and **D**), which revealed the in-plane WS_2 lattice fringe (i.e., top surface point **A**) and (002) SWCN side-wall fringes simultaneously. This is particularly evident in Fig. 2(a) where the (100) WS_2 lattice fringes, arising from the electron beam, scatter from the front and back of the WS_2 nanotube, which overlaps the (002) SWCN lattice fringes, causing a blurred appearance of the SWCN walls.

The template-controlled formation of WS_2 nanostructures via the $WO_3 \rightarrow WS_2$ conversion is now well substantiated.[5–8] In this study, it is likely that the WO_{3-x}-coated SWCNs act as precursors for WS_2 nanotube generation. That is, the $WO_{3-x} \rightarrow WS_2$ conversion occurs on SWCN surfaces during H_2S pyrolysis, resulting in the encapsulation of SWCNs within WS_2 nanotubes.

The authors thank the EPSRC, the Leverhulme Trust, the Royal Society and the Wolfson Foundation for financial support.

[1] R. Whitby, W. K. Hsu, C. B. Boothroyd, P. K. Fearon, H. W. Kroto, and D. R. M. Walton, Chem. Phys. Chem. **10**, 620 (2001).
[2] R. Whitby, W. K. Hsu, C. B. Boothroyd, H. W. Kroto, and D. R. M. Walton (unpublished).
[3] C. Journet, W. K. Maser, P. Bernier, A. Loiseau, M. L. de la Chapelle, S. Lefrant, P. Deniard, R. Lee, and J. E. Fischer, Nature (London) **388**, 756 (1997).
[4] D. Goldberg, Y. Bando, L. Bourgeois, K. Kurashima, and T. Sato, Carbon **38**, 2017 (2000).
[5] R. Tenne, L. Margulis, M. Genut, and G. Hodes, Nature (London) **360**, 444 (1992).
[6] Y. Feldman, G. Frey, M. Homyonfer, V. Lyakovitskaya, L. Margulis, H. Cohen, G. Hodes, J. Hutchison, and R. Tenne, J. Am. Chem. Soc. **118**, 5362 (1996).
[7] Y. Feldman, V. Lyakovitskaya, and R. Tenne, J. Am. Chem. Soc. **120**, 4176 (1998).
[8] L. Margulis, P. Dluzewski, Y. Feldman, and R. Tenne, J. Microsc. (Paris) **181**, 68 (1996).
[9] P. M. Ajayan, V. Ravikumar, and J. C. Charlier, Phys. Rev. Lett. **81**, 1437 (1998).
[10] F. Banhart and P. M. Ajayan, Nature (London) **382**, 433 (1996).